

Medium Effects in Parton Distributions*

William Detmold[†]

Department of Physics, College of William & Mary, Williamsburg, VA 23187, USA

Jefferson Lab, 12000 Jefferson Ave, Newport News, VA 23606, USA

E-mail: wdetmold@jlab.org

Huey-wen Lin

Department of Physics, University of Washington, Seattle, WA 98195, USA

E-mail: hwlin@phys.washington.edu

Understanding the effects of a background hadronic medium on hadronic observables is important in the context of hadron structure. Many experiments probing nucleon structure make use of nuclear targets and unraveling the modifications that ensue is a complex task. Using lattice QCD, we investigate the ab initio computation of hadron structure in a medium, focusing on the structure of the pion in a Bose-condensed gas of pions.

The XXIX International Symposium on Lattice Field Theory - Lattice 2011

July 10-16, 2011

Squaw Valley, Lake Tahoe, California

*NT@UW-11-32

[†]Speaker.

1. Introduction

An important part of our experimental understanding of hadron substructure is that hadrons in a medium are different to those in free space. The ‘‘EMC effect’’, the modification of the proton $F_2(x, Q^2)$ structure function inside a nucleus (as first observed in 1983 by the European Muon Collaboration [1]) is one of the most famous examples of medium sensitivity. This effect has been studied in many hadronic models with varying degrees of success (see Ref. [2] for a recent review) but an understanding from first principles is lacking. While the EMC effect and other such modifications of hadron properties are not *a posteriori* unexpected from the viewpoint of Quantum Chromodynamics (QCD), the complexity of QCD calculations involving nuclei has prevented the direct investigation of such effects. In QCD, we expect that medium modification is a ubiquitous feature of complex hadronic systems and, in these proceedings, we report on the study of a close analogue of the EMC effect, namely the modification of pion structure in the presence of a Bose condensed medium of pions.

Since hadronic structure is a low energy consequence of QCD, the only tool with which to perform *ab initio* studies is lattice QCD (LQCD). Lattice QCD is formulated in Euclidean space, so physics defined on the light-cone, such as that embodied in the parton distributions and structure functions of deep inelastic scattering, is very difficult to address directly (an alternate approach is suggested in Ref. [3]). However, through the Wilsonian operator product expansion (OPE), the Mellin moments, $\langle x^n \rangle_h(\mu) = \int_{-1}^1 dx x^n q_h(x; \mu)$, of the unpolarised quark distribution, $q_h(x; \mu)$, in a hadron h correspond to the forward matrix elements of local operators (μ is the renormalisation scale). Here, we focus on the leading twist, unpolarised operators and have

$$\langle h; p | \mathcal{O}_q^{\{\mu_0 \dots \mu_n\}} | h; p \rangle = \langle x^n \rangle_h p^{\mu_0} \dots p^{\mu_n}, \quad (1.1)$$

$$\mathcal{O}_q^{\{\mu_0 \dots \mu_n\}}(x) = \bar{q}(x) \gamma^{\{\mu_0} D^{\mu_1} \dots D^{\mu_n\}} q(x). \quad (1.2)$$

where $\{\dots\}$ indicates symmetrisation of enclosed indices and subtraction of traces. The dependence of the various quantities on the renormalisation scale is suppressed for concision and q represents a particular flavour of quark field. The hadron h can be a proton or pion or it can be a more complex object such as a nucleus or a collection of mesons. In these proceedings, matrix elements of the $n = 1$ operator are investigated in systems of up to twelve pions.

2. Lattice Methods

These matrix elements can be computed using the lattice approach by measuring two- and three- point correlation functions in the appropriate hadronic states. For clarity, we will consider the case of the up quark distribution of the π^+ ($u\bar{d}$) in a medium of π^+ 's. Two point functions from a source location $x_0 = (\mathbf{x}_0, t_0)$,

$$C_m(t, \mathbf{p}) = \langle 0 | \left[\prod_{i=1}^m \sum_{\mathbf{x}} e^{i\mathbf{p}_i \cdot \mathbf{x}} \pi^+(\mathbf{x}, t) \right] [\pi^-(x_0)]^m | 0 \rangle, \quad (2.1)$$

where $\pi^+ = \bar{u}\gamma_5 d$, allow the energies of systems of m -pions to be determined from the dependence on Euclidean time. The total momentum of the m -pion state is $\mathbf{p} = \sum_{i=1}^m \mathbf{p}_i$ as selected by the

summations over spatial sink locations (the individual \mathbf{p}_i are not quantum numbers). In the current context, we shall only consider $\mathbf{p} = \mathbf{0}$.

For $t_0 = 0$, the spectral decomposition of the correlator has the form [4]

$$C_m(t, \mathbf{0}) \rightarrow \sum_{\ell=0}^m \binom{m}{\ell} Z_m^{(\ell)} e^{-E_{m-\ell}t} e^{-E_\ell(T-t)} + \dots, \quad (2.2)$$

where T is the temporal extent of the lattice and the ellipsis denotes excited states that are exponentially suppressed as t increases. The factors $Z_m^{(\ell)} \sim |\langle \ell | (\pi^+)^m | m - \ell \rangle|^2$ represent the overlap of the m -pion interpolating operator onto $(m - \ell)$ π^+ 's going forward in time and ℓ π^- 's going backward in time (in the ground state, the momentum of the forward and backward going collections of pions separately vanish). Note that $Z_m^{(m-\ell)} = Z_m^{(\ell)}$. In the limit of a large temporal extent of the lattice ($T \rightarrow \infty$), only the term with $\ell = 0$ contributes, but at finite T (corresponding to non-zero temperature), thermal states in which some number of pions travels around the temporal boundary are important as we shall see below.

Corresponding three point correlation functions allow the matrix elements in Eq. (1.1) to be determined for the operator $\mathcal{O}_q^{(n)} \equiv \mathcal{O}_q^{\{\mu_0 \dots \mu_n\}}$,

$$C_m^{(n)}(\tau, t, \mathbf{p}) = \langle 0 | \left[\prod_{i=1}^m \sum_{\mathbf{x}} e^{i\mathbf{p}_i \cdot \mathbf{x}} \pi^+(\mathbf{x}, t) \right] \sum_{\mathbf{y}} \mathcal{O}_u^{\{\mu_0 \dots \mu_n\}}(\mathbf{y}, \tau) [\pi^-(x_0)]^m | 0 \rangle. \quad (2.3)$$

Here, the operator is inserted at time-slice τ injecting zero momentum. The spectral decomposition of the three point correlator for $\mathbf{p} = \mathbf{0}$ is

$$C_m^{(n)}(\tau, t, \mathbf{0}) = \sum_{\ell=0}^m \binom{m}{\ell} Z_m^{(\ell)} \langle \mathcal{O}_{m-\ell}^{(n)} \rangle e^{-E_{m-\ell}t} e^{-E_\ell(T-t)} + \dots, \quad (2.4)$$

and $\langle \mathcal{O}_m^{(n)} \rangle = \langle m | \mathcal{O}_u^{(n)} | m \rangle$ is the matrix element of the operator in the m -pion state. Excited states are suppressed in this expression and we assume $\langle \mathcal{O}_0^{(n)} \rangle = 0$ for the cases we consider. For m -pion systems, contributions involving colour singlet sub-states propagating around the temporal boundary result in there being contributions from matrix elements of states with $\ell < m$ pions. Near the middle of the temporal extent, $t \sim T/2$, these contributions may be important.

In the large T limit, only the $\ell = 0$ state contributes in Eqs. (2.2) and (2.4) and it is clear that the ratio

$$\begin{aligned} R_m^{(n)} &= \frac{C_m^{(n)}(\tau, t, \mathbf{0})}{C_m(t, \mathbf{0})} \longrightarrow \langle m | \mathcal{O}_u^{\{\mu_0 \dots \mu_n\}}(\mu) | m \rangle \\ &= p^{\mu_0} \dots p^{\mu_n} \langle x^n \rangle_{m\pi}(\mu), \end{aligned} \quad (2.5)$$

where $p^\mu = (\mathbf{0}, E_m)$. This ratio will be independent of the sink and operator insertion times, t and τ , provided $t_0 \ll \tau$, $|t - \tau| \ll T$ and determines the in-medium Mellin moment. It follows that the double ratio $\mathcal{R}_m^{(n)} = R_m^{(n)} / R_1^{(n)}$ determines the ratio of moments in medium to those in free space that we are interested in up to a simple kinematic factor. This double ratio is independent of the renormalisation scale, μ , obviating the need for calculating the coefficients necessary to match lattice operators to operators in the $\overline{\text{MS}}$ scheme. If $t - t_0$ is not much less than T , the above ratios

Label	a [fm]	$L^3 \times T$	m_π [MeV]	$m_\pi L$	$m_\pi T$	Measurements
F	0.09	$28^3 \times 96$	320	4.1	14.0	432
C1	0.12	$20^3 \times 64$	290	3.7	11.7	1450
C2	0.12	$20^3 \times 64$	350	4.4	14.2	837
C3	0.12	$20^3 \times 64$	490	6.2	19.9	1000
L	0.12	$20^3 \times 64$	350	6.3	14.2	250

Table 1: Details of measurements and ensembles used in this calculation. For each data set, the remaining columns correspond to the lattice spacing, lattice dimensions, valence pion mass and number of configurations \times number of sources on each configuration.

will be contaminated by thermal contributions. However, Eqs. (2.4) and (2.2) can still be used to extract the Mellin moments $\langle x^n \rangle_{m\pi}(\mu)$.

In terms of a lattice calculation, the two and three point functions we require are complicated by the many Wick contractions that arise in multi-pion systems. We proceed by defining partly contracted objects

$$\begin{aligned} \Pi(t; \mathbf{p}) &= \sum_{\mathbf{x}} S_u(\mathbf{x}, t; \mathbf{x}_0, t_0) S_d^\dagger(\mathbf{x}, t; \mathbf{x}_0, t_0), \\ \widehat{\Pi}^{(n)}(t, \tau; \mathbf{p}) &= \sum_{\mathbf{x}, \mathbf{y}} e^{i\mathbf{p} \cdot \mathbf{x}} S_u(\mathbf{y}, \tau; \mathbf{x}_0, t_0) \gamma_5 \gamma^{\{\mu_0} D^{\mu_1} \dots D^{\mu_n\}} \gamma_5 S_u(\mathbf{x}, t; \mathbf{y}, \tau) S_d^\dagger(\mathbf{x}, t; \mathbf{x}_0, t_0), \end{aligned}$$

where S_q is the quark propagator of flavour q and we have used γ_5 -hermiticity, $S(x, y) = \gamma_5 S^\dagger(y, x) \gamma_5$, to reverse the arguments of propagators from sink to source and contraction on spin and colour indices is assumed. These objects can be viewed as time-dependent 12×12 matrices in spin and colour space. Using the techniques developed in Refs. [4, 5, 6, 7], the required contractions can now be built in terms of spin-colour traces of products of these matrices that can be efficiently computed. As the multi-hadron correlators decay very rapidly with Euclidean time, high precision arithmetic is needed in these calculations for which we use the QD library [8].

Numerical details: Our calculations are performed using gauge configurations generated by the MILC collaboration [9] using the rooted-staggered formulation of quarks and the asqtad gauge action. One level of HYP smearing [10] is applied to these configurations to reduce short distance fluctuations. The ensembles used in this study are shown in Table 1, where we also report the number of configurations used and the number of source locations used on each configuration (the L ensemble has been used solely for checks of volume dependence). Domain-wall [11, 12] valence quark propagators have been calculated from APE smeared [13] sources at various locations by the NPLQCD and LHP collaborations [14, 15]. These are then APE smeared on the sink time-slice with fixed momentum and used as the source for the sequential propagators connecting to the operator generated using the same action. The source–sink separation in the three point correlation functions is chosen at $t_{\text{sep}}/a \equiv (t - t_0)/a \in \{16, 20, 24, 28, 32\}$ on the C1, C2 and C3 ensembles and at $t_{\text{sep}}/a \in \{24, 32, 48\}$ on the F ensemble. The operator insertion time is varied over the entire lattice.

3. Thermal contamination

A major issue in the present calculations is the contribution of thermal states to two- and three-

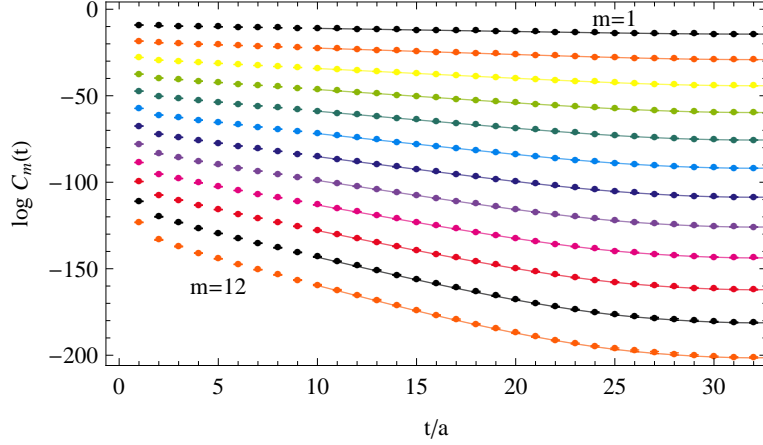


Figure 1: The logarithm of the correlators for the $m = 1, \dots, 12$ pion systems on the C1 ensemble. Also shown are the fits to these correlators and their uncertainties.

point correlations functions. Given that the temporal extent of the lattice is fixed, one needs to go to early Euclidean times in order to ensure that the true ground state of the system is dominating the signal. However at early time, one must be concerned about (forward-going) excitations that are damped at later Euclidean times and a careful analysis is required. By using the full form of the expected correlator, Eq. (2.2), and performing fits to all 12 correlators, the energies E_m and the multiple overlap factors $Z_m^{(\ell)}$ can be determined. Since we successively fit C_1, C_2, \dots, C_{12} , only a single energy is determined by each fit and to account for correlations we perform these fits using a bootstrap procedure. The results of our fits to the correlators on the C1 ensemble are shown in Fig. 1.

The extracted bootstrap sets of parameters can then be used to reconstruct the correlator in the limit of infinite temporal extent by removing all thermal contributions. In Fig. 2, the ratios of these zero temperature extrapolation of the correlators to the original correlators are shown as a function of Euclidean time for the $m = 1, \dots, 12$ pion systems (again for the C1 ensemble). It is clear from this figure that for source–sink separations beyond $t \sim 20$, it will prove difficult to extract the m -pion matrix element from the corresponding three-point function as the desired contribution will be suppressed relative to the thermal contributions. This is also the case for the C3 ensemble (where $m_\pi T \sim 20$) for larger numbers of pions as shown in the right panel of the figure.

4. Quark momentum fraction

In order to perform extractions of the matrix elements, we use the bootstrap list of the m -pion energies and overlap factors obtained from the two-point functions and input them into the expected spectral decomposition of the three-point function, Eq. (2.4). Using multiple different source–sink separations, we then fit the parameters $\langle \mathcal{O}_m^{(n)} \rangle$ to the three point data under the bootstrap procedure. In Fig. 3, we show preliminary results for the the dependence of $\langle x \rangle_{m\pi}$ on the density of the pion gas for the C3 ensemble. Mild dependence on the density of pions is observed but further work remains to better quantify systematic effects and to study the dependence on quark masses and the continuum and infinite volume limits.

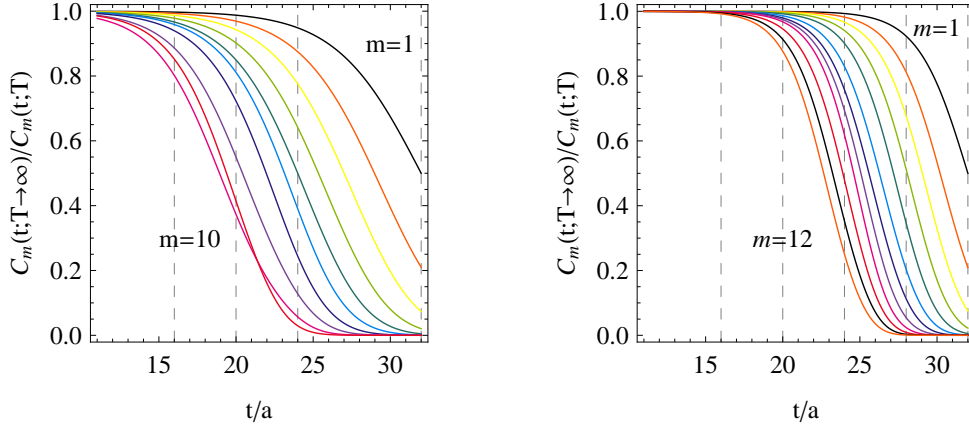


Figure 2: The ratio of the zero temperature reconstruction of the correlators for $m = 1, \dots, 12$ pion systems to the fitted (finite T) correlators. Data are from the C1 (left) and C3 (right) ensembles. When this ratio deviates from unity, thermal effects are making significant contributions to the correlator.

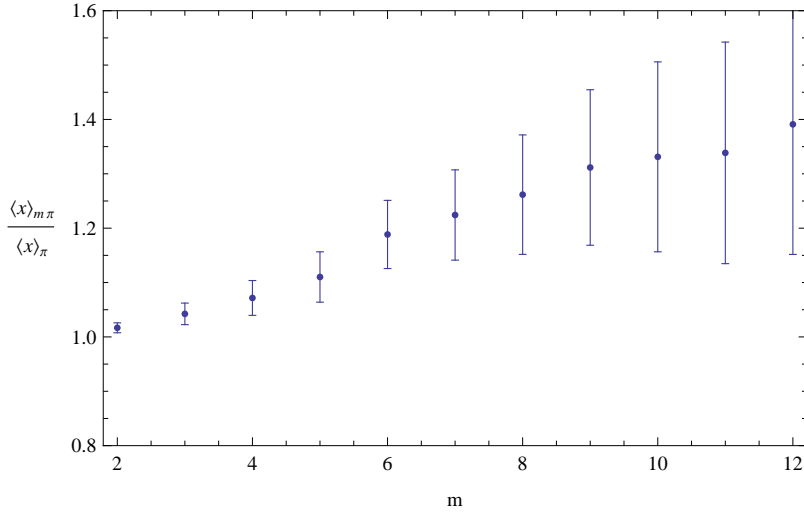


Figure 3: Extracted ratio of pion momentum fraction in an m -pion system to that in a single pion, $\langle x \rangle_{m\pi} / \langle x \rangle_\pi$ for the C3 ensemble as a function of the number of pions in the system.

5. Discussion

It is clear from our preliminary studies presented here that the investigation of multi-hadron matrix elements is a challenging task in lattice QCD. While the current investigations focus on multi-pion systems, similar techniques in principle allow access to matrix elements in nuclei. With the recent observation of bound light nuclei in quenched QCD [16, 17] and QCD at unphysical quark masses [18, 19, 20, 21], further studies are warranted. However, the large statistics needed in lattice studies of few-body nuclei make this a daunting task for the future. On a more positive note, the thermal contamination that has hampered then current investigations is particularly vexing as $E_{m-\ell} + E_\ell < E_m$ for these systems and in light nuclei, where the binding per nuclei increases, this may not be such a significant issue.

Acknowledgments

We thank D. B. Kaplan, S. Meinel, K. Orginos, M. J. Savage and J. Zanotti for useful discussions, the MILC, NPLQCD and LHP collaborations for access to gauge configurations and propagators, and R. Edwards and B. Joo for the development of the `chroma` library [22]. The work of HWL was supported by the U.S. Department. of Energy (DOE) grant DE-FG03-97ER4014, and that of WD in part by Jefferson Science Associates, LLC under DOE contract No. DE-AC05-06OR-23177, DOE grants DE-FG02-04ER41302 and DE-SC000-1784, and by the Jeffress Memorial Trust (J-968). Computing support was provided by NERSC (DE-AC02-05CH11231) and the Hyak cluster at the University of Washington eScience Institute, using hardware awarded by NSF grant PHY-09227700. .

References

- [1] J. Aubert et al., *Phys.Lett.* **B123**, 275 (1983).
- [2] P. Norton, *Rept.Prog.Phys.* **66**, 1253 (2003).
- [3] W. Detmold and C. Lin, *Phys.Rev.* **D73**, 014501 (2006).
- [4] W. Detmold and B. Smigielski, *Phys.Rev.* **D84**, 014508 (2011).
- [5] S. R. Beane et al., *Phys.Rev.Lett.* **100**, 082004 (2008).
- [6] W. Detmold et al., *Phys.Rev.* **D78**, 014507 (2008).
- [7] W. Detmold and M. J. Savage, *Phys.Rev.* **D82**, 014511 (2010).
- [8] D. H. Bailey, Y. Hida, X. S. Li, and B. Thompson,
<http://crd-legacy.lbl.gov/~dhbailey/mpdist/>.
- [9] C. W. Bernard et al., *Phys.Rev.* **D64**, 054506 (2001).
- [10] A. Hasenfratz and F. Knechtli, *Phys.Rev.* **D64**, 034504 (2001).
- [11] D. B. Kaplan, *Phys.Lett.* **B288**, 342 (1992).
- [12] V. Furman and Y. Shamir, *Nucl.Phys.* **B439**, 54 (1995).
- [13] M. Albanese et al., *Phys.Lett.* **B192**, 163 (1987).
- [14] S. Beane et al., 1108.1380.
- [15] A. Walker-Loud et al., *Phys.Rev.* **D79**, 054502 (2009).
- [16] T. Yamazaki, Y. Kuramashi, and A. Ukawa, *Phys.Rev.* **D81**, 111504 (2010).
- [17] T. Yamazaki, Y. Kuramashi, and A. Ukawa, *Phys.Rev.* **D84**, 054506 (2011).
- [18] S. R. Beane et al., *Phys.Rev.* **D80**, 074501 (2009).
- [19] S. Beane et al., *Phys.Rev.Lett.* **106**, 162001 (2011b).
- [20] T. Inoue et al., *Phys.Rev.Lett.* **106**, 162002 (2011).
- [21] S. Beane et al., 1109.2889.
- [22] R. G. Edwards and B. Joo, *Nucl.Phys.Proc.Suppl.* **140**, 832 (2005).